INTERNATIONAL ATOMIC ENERGY AGENCY
UNITED NATIONS EDUCATIONAL, SCIENTIFIC AND CULTURAL ORGANIZATION

INTERNATIONAL CENTRE FOR THEORETICAL PHYSICS
34100 TRIESTE (ITALY) - P.O.B. 586 - MIRAMARE - STRADA COSTIERA 11 - TELEPHONE: 2240-1
CABLE: CENTRATOM - TELEX 460892-1

SMR/388 - 46

SPRING COLLEGE IN MATERIALS SCIENCE
ON
'CERAMICS AND COMPOSITE MATERIALS'
(17 April - 26 May 1989)

RADIATION EFFECTS IN CERAMICS

G.P. PELLS
United Kingdom Atomic Energy Authority
Harwell Laboratory - Materials Development Division
Oxon
Didcot OX11 ORA
United Kingdom

RADIATION EFFECTS IN CERAMICS

G.P. Pells

Harwell Laboratory,

Oxon. OX11 ORA

U.K.

May 1989

Radiation Effects in Ceramics

Defects in Crystals

We shall first consider how solids depart from perfection in one way or another.

A defect in a solid is defined as any deviation from the perfectly ordered crystal lattice.

Point Defects

The simples defect is a vacancy which is a site in the crystal lattice where there is a missing atom or ion.

The complemtary defect to a vacancy is an interstitial, an extra atom or ion inserted at a site where there is not normally an atom or ion. These extra sites are called insterstitial sites.

An isolated vacancy in a crystal is known as a Schottky defect and the complementary pair of an interstitial and a vacancy is a Frenkel defect or Frenkel pair.

Under some conditions groups of vacancies or interstitials may come together to form aggregates.

as defects

Impurities may also be regarded in the crystal structure. Isolated impurity atoms may occupy substitutional or interstitial sites. Sometimes groups of impurity atoms or even the precipitation of a second phase may occur.

Impurities are often called extrinsic defects while vacancies and interstitials are called intrinsic defects.

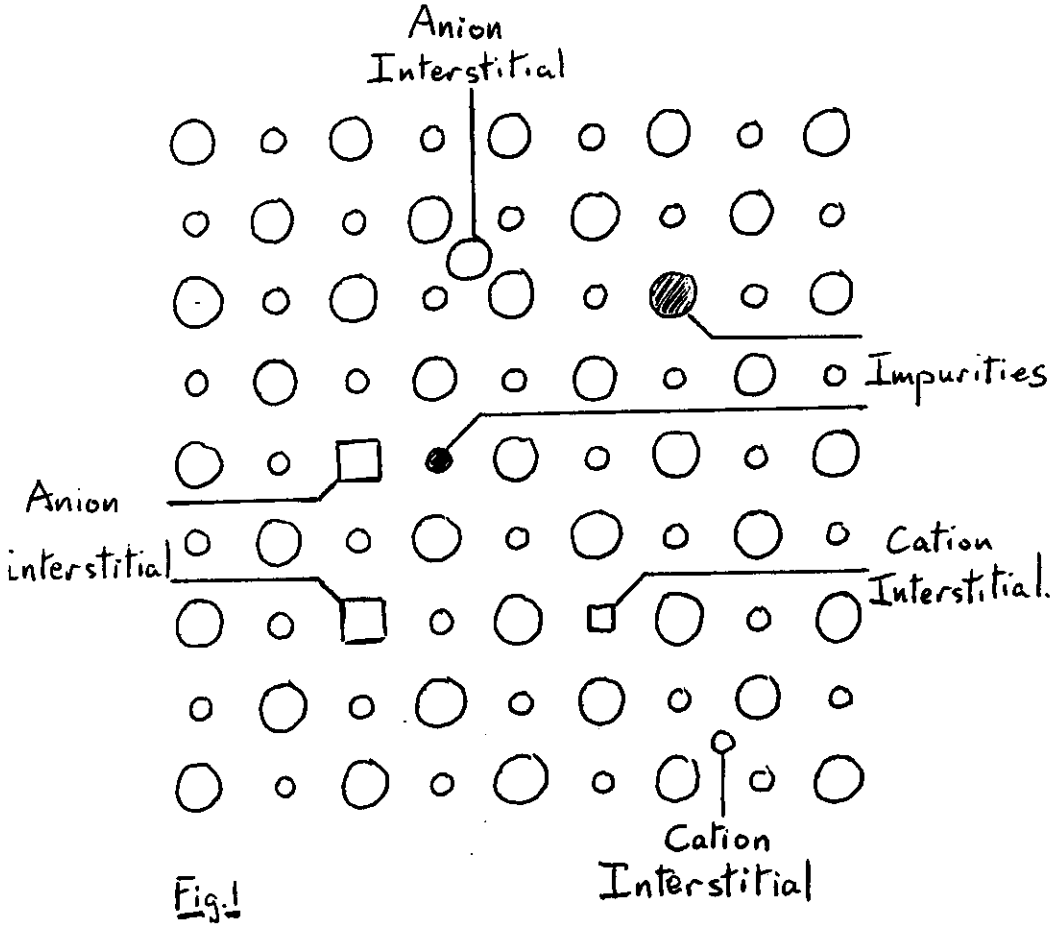

Fig.1

Pre-existing dislocations may act as sinks for vacancies and interstitials produced by radiation damage.

New dislocations may also be produced by the aggegation of vacancies or interstitials to form dislocation loops. These are extra or missing planes of atoms which extend through only a limited part of the crystal. In alkali halides and oxides dislocations involve extra planes of both cations and anions in order to preserve electrical neutrality.

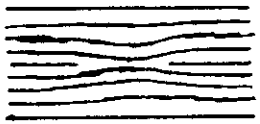

vacancy loops

interstitial loops

Grain boundaries in plycrystalline materials

As the mismatch between adjacent grains widens a greater number of dislocations are required to accommodate the mismatch. Above an included angle of 30° the separation between dislocations becomes of the order of an interatomic spacing. The structure of a large angle boundary is thought to be like a thin amorphous layer between the two grains of a few atom layers thickness.

Origins of Defects

Chemical

Chemical impurities may be held in solid solution or they may exceed the solubility limit and ppt out as separate compounds (or phase). The solubility limit usually increases with increasing temperature.

Impurities may give rise to other defects such as vacancies or interstitials. This is particularly marked in ionic crystals. If the impurity has a different valency to the host ion that it replaces the other defects are introduced to compensate the different charge.

Consider a Ca^{2+} impurity on NaCl. The NaCl is ionised to Na^+ and Cl^- therefore substitutional Ca^{2+} gives an extra charge. This is compensated by leaving a Na^+ site empty and so introduce a positive ion (cation) vacancy. The Ca^{2+} could be charge compensated by a Cl^- interstitial but this is a large ion and is energetically unfavourable.

The empty cation vacancy represents a missing positive ion and therefore behaves as if it had a negative charge with respect to the perfect lattice. It is thus attracted to a site next to the Ca^{2+} ion giving an impurity-vacancy pair.

Some structures such as the close packed hexagonal lattice of α-Al_2O_3 can only telerate small numbers of impurity atoms with different valencies before the impurity precipitates out as a second phase. Others such as the cubic spinel structure can accommodate wide variations in impurity content and stoichiometry. In the perfect spinel structure local charge neutrality is maintained by divalent cations occupying tetrahedral sites and trivalent cations occupying octahedral sites. Interchange of divalent and trivalent cations produce antistructure defectswhich in synthetic $MgAl_2O_4$ are typically 10-15%. The antistructure defects introduce centres of local positive and negative charge as an Al^{3+} on Mg^{2+} site, $[Al]^{+}_{mg}$, is a site with excess positivecharge. Similarly Mg^{2+} on an Al^{3+} site, $[Mg]^{-}_{Al}$, is a site with excess negative charge.

In UO_2 with excess oxygen the extra O_2 ions are incorporated interstitially, since UO_2, which has the fluorite structure, has some large interstitial spaces.

Creation of Defects by Radiation

Defects may be created in solids by the interaction of the lattice atoms with a large range of energetic irradiating particles including photons, charged particles and neutrons. The majority of techologically important radiation effects are caused by charged particles and neutrons producing atom-atom collisions. However, the most efficient radiation damage process called Radiolysis occurs by an ionisation process in a limited number of materials.

Although displacement damage may be produced by several types of radiation there are a number of features common to all damage sequences and to a first approximation it may be stated that the majority of damage is produced by momentum transfer from a projectile to a target atom which then itself goes on to make further collisions with lattice atoms.

Radiolysis is a somewhat special case and will be dealt with first.

Radiolysis

When a charged particle or high energy photon interacts with a material excitation of valence electrons is the primary process which occurs. There are then four criteria for efficient coupling of the electronic interaction to atomic displacement phenomena.

1) the electronic excitation must be localized to one or at most a few atom sites;

2) the excitation must have a lifetime (10^{-13}s) comparable with lattice vibrations in order to couple into a mechanical response of nuclear masses;

3) the available excitation energy must be comparable to the atom displacement energy in its excited state T_d

4) an energy to momentum conversion mechanism must exist which can compete favourably with other excitation decay modes such as recombination luminescence.

The above criteria are satisfied by single electron excitations in wide band gap insulators forming bound electron-hole (self-trapped exciton) states.

Initially an electron is excited from a X^- ion into the conduction band after which it may recombine immediately with a hole or become trapped at an impurity or crystal defect. The hole that is left behind is trapped between two halide ions which relax to form an $[X_2^-]^+$ molecule or V_K centre. (The self-trapped hole is mobile with an activation energy of 0.3eV.) The $[X_2^-]^+$ centre may also trap a self-trapped exciton. The formation of a Frenkel pair involves the radiationless dissociation of the self-trapped exciton along a close-packed <110> direction. The X_2^- molecule moves away from the initial exciton site. The dissociation occurs in a few picoseconds (10^{-12}s) leaving the electron in the ground state of the resulting vacancy [F centre] and an interstitial halide ion removed some distance from the vacancy as an X_4^{3-} crowdion (H centre).

Radiolysis does not occur in highly ionic oxides but does occur in alkaline earth halides, silica and silicates.

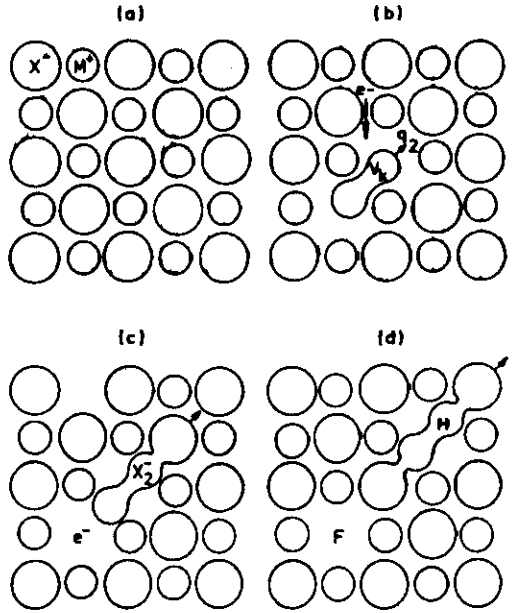

AERE - R 7929 Fig. 3

Sequence of Frenkel pair production by radiolysis. (a) Initially perfect lattice. (b) Self-trapped hole (V_k centre) formed by ionisation recombines with an electron to form a self-trapped exciton which can dissociate. (c) X_2^- part of the self-trapped exciton departs in an excited state along q_2 coordinate, leaving electron behind in the ground state of the resulting vacancy (F centre). (d) X_4^{3-} crowdion interstitial (H centre) forms at some distance from the F centre.

Defects Produced by Momentum Transfer

Atoms may be displaced from their normal position by collision with an energetic particle having sufficient momentum. In the case of photons such as gamma rays the interaction is indirect as the photon first excites an electron which, if sufficiently energetic, may then go on to displace an atom.

There are two concepts fundamental to displacement damage:

1) The displacement cross-section - the probability of a moving particle colliding with a lattice atom.

2) The displacement threshold energy - the minimum energy required to displace an atom from its (normal) lattice position.

The Displacement Threshold Energy E_d

The concept of a displacement threshold energy follows from the simple idea by Seitz that an energy equal to 4 times the sublimation energy of the atoms in a crystal must be provided to permanently displace an atom from its normal lattice site (20-25eV). An accurate value for E_d is a necessary requirement of any calculation of the number of atoms displaced by irraidation.

E_d may be measured using monoenergetic electrons of ~ 1MeV so that only 1 atom is displaced per collision. The minimum kinetic energy of the electrons required to produce a radiation sensitive property change is determined and thus E_d deduced from the relativistic equation

$$E_d = \frac{2E_{min}\left[E_{min} + 2m_e c^2\right]}{M_2 c^2} \qquad (1)$$

where E_{min} is the minimum electron energy required to displace a lattice atom, m_e is the mass of the electron, c is the velocity of light and M_2 is the mass of the displaced atom.

In ceramics the displacement threshold energy will depend on bond strengths, which may be quite large for ionic solids, and on the space available to accommodate an interstitial atom in a close-packed structure. The interstitial may be limited to a restricted number of sites due to the electrostatic repulsion of a charged interstitial giving displacement energies several times the binding energy.

In covalent solids the directed nature of the bonding results in less close-packed structures and displacement energies are closer to bonding energies.

The effect of crystal structure may be illustrated by the very low energy required to displace the aluminium ion in alumina which has been shown to have an E_d^{Al} of 18eV whereas the oxygen ion has an E_d^{O} of 76eV. This is probably due to the defect nature of Al_2O_3 where one third of the aluminium lattice sites are unoccupied and therefore available to accept a displaced Al ion.

Although most damage calculations assume an abrupt displacement threshold it is unlikely to be a step function due to orientation anisotropy, channeling of the displaced atom and the probabilistic nature of close Frenkel pair recombination. Although E_d has been shown experimentally to vary with crystallographic orientation by relatively small amounts, computer calculations of E_d along close packed directions in single cubic structures give values of $E_d > 100$eV.

Table 1 gives experimental values of E_d for some common ceramic materials.

The effects of differing ion mass and displacement threshold energy on the relative number of displacements made by each atom in multicomponent materials has been calculated and it has been found that large variations could occur when E_d varies significantly between the different species. For instance in α-Al_2O_3 approximately three Al atoms are displaced for each oxygen atom.

Table 1
Values of displacement threshold energy, E_d, for some insulating ceramics

Material	Element and orientation	E_d (eV)	Average E_d (eV)	
BeO	Be	~ 20	50	
	O	76		
MgO	Mg ⟨001⟩	60 ± 3	60	56
	⟨011⟩	60 ± 3		
	⟨111⟩	60 ± 3		
	O ⟨001⟩	44 ± 3	53	
	⟨011⟩	64 ± 3		
	⟨111⟩	46 ± 3		
Al_2O_3	Al random	18 ± 3	20	50
	O random	76 ± 3	65	
	random	90		
	⟨0001⟩	53		
	⟨11$\bar{2}$0⟩	41		
$MgAl_2O_4$	Mg ⟨001⟩	20	30	45
	Mg	30		
	Al	30		
	O	59		
$Al_{23}O_{27}N_5$			~ 50	
AlN			~ 50	
Si_3N_4			~ 50	

Displacement Cross-sections

We shall now consider the displacement cross-sections for several types of irradiating particle. Early work showed that collision cross-sections, σ, were commonly of the order of 10^{-24} cm^2. This unit was called a 'barn'.

Displacement damage processes vary widely in detail depending upon the nature of the irradiating particle but nearly all involve momentum transfer to a lattice atom which acquires sufficient energy for itself to be regarded as an irradiating particle, a primary knock-on atom or PKA. For this reason we shall first consider the damage mechanisms involved in ion irradiation.

Ions

Ions and atoms of sufficiently high velocity will be stripped of some of their outer electrons as they enter the solid. Above a certain energy, which increases with increasing atomic number Z, the moving ion loses energy predominantly by collision with electrons and so leaves a core of excited electrons and ionised atoms along its path. The nucleus of the moving ion may also interact with a nucleus of the target via the coulomb potential in a Rutherford scattering event, but such collisions are predominantly at glancing angles which do not give large momentum transfers.

The cross-section for Rutherford scattering d (E) in which energy E is transferred to the initially stationary atom is given by:

$$d\sigma(E) = \frac{\pi b^2}{4} \cdot \frac{E_m}{E} \cdot dE \qquad (2)$$

where b is the distance of closest approach given by

$$\frac{Z_1 Z_2 e^2}{b} = \left(\frac{M_1 M_2}{M_1 + M_2}\right)\frac{V^2}{2} \qquad (3)$$

with V being the velocity of the moving ion.

$$E_{max} = \frac{4 M_1 M_2}{(M_1 + M_2)^2} \cdot E \qquad (4)$$

The cross-section for primary displacement is the integral of this cross-section from E_d to E_m and is

$$\sigma_d = \frac{\pi b^2}{4}\left[\frac{1}{E_d} - \frac{1}{E_m}\right] E_m \qquad (5)$$

The mean energy transferred to the struck atom is

$$E_s = E_d \ln\left[\frac{E_m}{E_d}\right] \quad \text{for } E_m \gg E_d \qquad (6)$$

so that in general E_s is of the order of a few hundred electron volts.

The knock-on atoms produced by the Rutherford collisions are sufficiently energetic to produce a few further displacements.

Assuming that a knock-on atom with energy E_s will produce $E_s/2E_d$ further displacements for $E_s > 2E_d$ and only one displacement for $E_d < E_s < 2E_d$ then the average total number of displacements n_d produced in a Rutherford collision is

$$n_d = 0.5 \left\{ 1 + \ln \left(\frac{E_m}{2E_d} \right) \right\} \qquad (7)$$

As the energy of the moving ion falls even further it approaches closer to the condition of a neutral atom at which point further interactions are essentially elastic collisions between the electron clouds of the moving atom and the target. The energy at which the moving atom begins to suffer elastic collisions is given by the approximate relationship

$$L_c = \frac{1}{8} \cdot \frac{M I}{m_e} \text{ , in eV ,} \qquad (8)$$

where I is the band gap in an insulator. The hard-sphere collisions at the lower end of the energy range are those which produce the majority of atomic displacements.

The partitioning of displacement mechanisms with energy of the moving atom has been described by Kinchin and Pease.

It is assumed that any atom given an energy in excess of E_d is displaced, but only an atom with energy $>2E_d$ can make a collision with a target atom after which both have an energy exceeding E_d. Thus atoms with energies between E_d and $2E_d$ are displaced but cannot themselves cause further displacements.

If the moving atom has energy E between $2E_d$ and L_c then it may be shown that the number of displaced atom $N_d = E/2E_d$.

Thus we may divide the number of atoms $\nu(E)$ displaced by an atom receiving an energy E into four ranges:

$$\nu(E) = \begin{cases} 0 & E < E_d \\ 1 & E_d \leq E < 2E_d \\ E/2E_d & 2E_d \leq E < L_c \\ L_c/2E_d & E \geq L_c \end{cases} \qquad (9)$$

G.H. Kinchin and R.S. Pease
Rep. Prog. Phys. 18 (1955)

From these simple concepts we may go onto calculate the numbers of atoms displaced by other irradiating particles.

Neutrons

The displacement of atoms in solids by neutron irradiation occurs by two somewhat different mechanisms. In the first neutron collides with the nucleus of an atom and imparts to it on energy in excess of E_d. The displaced target atom may well have sufficient energy to produce further displacements by the mechanisms discussed previously. The second mechanism concerns thermal neutron capture leading to a transmutation event.

In general high energy neutrons suffer elastic collisions with target nuclei in which case the maximum energy E_m which may be transferred by a neutron of energy E_n to a nucleus of atomic weight M is

$$E_m = \frac{4M}{(M+1)^2} \cdot E_n \qquad (10)$$

The struck nucleus has an equal probability of receiving any energy between zero and E_m, therefore the average energy transferred in such collisions is $E_m/2$.

If the atomic cross-section for elastic scattering of a neutron of energy E_n by a target nucleus is $\sigma(E_n)$ then the number of collisions occurring in unit volume of the solid with a flux of monoenergetic neutrons F for time t

$$N = N_o F t \sigma (E_n) \qquad (11)$$

where N_o is the number of atoms per unit volume. The product $Ft=\phi$ is called the fluence.

The primary knock-on atoms (PKA) produced by collision with neutrons are generally sufficiently energetic to produce further displacements. The PKA will produce further displacements as described by the Kinchen and Pease relationships in equation 9. The average number of displacements is

$$\bar{\nu} = \frac{L_c}{4E_d}\left[2 - \frac{L_c}{E_m}\right] \qquad (12)$$

Therefore the total number of displacements per unit volume for a fluence ϕ of neutrons with energy E_n is

$$N = N_o \phi \sigma (E_n) \nu \qquad (13)$$

Collision Cascades

Both neutron and heavy-ion collisions lead to the concept of a collision cascade which occurs when the moving particle becomes an atom (below L_c) and suffers hard-sphere collisions with lattice atoms with a reasonable probability that each collision will result in a displaced atom which itself goes on to displace other atoms and so on. The net result of this sequence of multiple collisions is that atoms are displaced outwards from the PKA to give vacancy lattice sites at the centre of the cascade. The fate of the vacancies and interstitials will be discussed later.

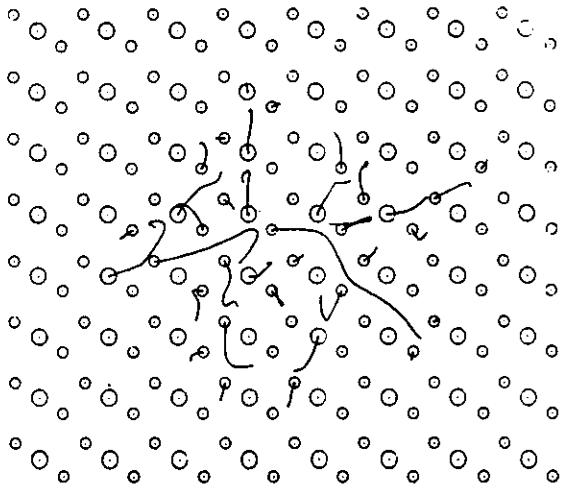

Fig. 5

Electrons

Energetic electrons are able to produce displacements by direct interaction with the nuclei of the solid through the Coulomb potential. The nuclear masses are so much greater than that of the electron that momentum transfer will only be sufficient to displace a few atoms. This is often a useful attribute in radiation damage research such as the measurement of the displacement threshold energy E_d.

In order to calculate the number of atoms displaced by electron irradiation we require the displacement cross-section σ_d of the nuclei for the incident electron whose energy must be treated using relativistic mechanics.

The kinetic energy of an electron is given by

$$E = m_e c^2 \left[\left(\frac{1}{\left(1 - \left|\frac{V}{c}\right|^2\right)^{\frac{1}{2}}} \right) - 1 \right] \qquad (14)$$

where V is the velocity of the electron
c is the velocity of the light
and m_e is the rest mass of the electron

The maximum possible energy transfer is:

$$E_m = \frac{2m_e}{M} \cdot \frac{(E + 2m_e c^2)}{m_e c^2} \cdot E \qquad (15)$$

Then the displacement cross-section is given by the McKinley and Feshbach equation

$$\sigma_d = \frac{\pi}{4}\left(\frac{b}{\gamma}\right)^2\left[\left(\frac{E_m}{E_d} - 1\right) - \beta^2 \ln\left(\frac{E_m}{E_d}\right) + \pi\alpha\beta\left\{2\left[\left(\frac{E_m}{E_d}\right)^{\frac{1}{2}} - 1\right] - \ln\left(\frac{E_m}{E_d}\right)\right\}\right] \qquad (16)$$

where

$$b = 2Ze^2 / m_e c^2$$

$$\gamma = (1-\beta^2)^{-\frac{1}{2}}, \quad \beta = v/c$$

$$\alpha = Z/137$$

The PKA will have energies below L_c, the threshold for hard sphere collisions, so that the total number of displacements

$$n = 0.56\left(1 + \frac{E_m}{E_d}\right) \qquad (17)$$

In recent years powerful computer codes have been developed to calculate the partitioning of the energy of an irradiating particle into electronic excitation and into displacement damage taking into account realistic interatomic potentials, displacement threshold effects, crystal lattice structure and temperature.

A statistical description of energy loss by knock-on atoms was formulated by Linhard et al. and subsequent development of the Kinchin and Pease relationships by Norgett, Robinson and Torrens (NRT) lead to an equation for the number of Frenkel pairs

$$N_d = \frac{k(E_p - Q)}{2E_d} = \frac{kE}{2E_d} \qquad (18)$$

where Q is the total energy lost in the cascade by electron excitation, E is the damage energy available for atomic displacement and K is the displacement efficiency which is usually taken to be 0.8.

Commonly available computer codes for calculating damage are RECOIL for neutron irradiation, E-DEP-1 and TRIM (a Monte Carlo program) for heavy ion irradiations.

M.D. Matthews, AERE R-10848 (1983)
J.P. Biersack, Z. Phys., A305 (1982) 95

Of the two constants k and E_d that go into the computer calculations those for E_d are reasonably well established. However recent work has shown that the damage efficiency, instead of having a constant value of k=0.8, may vary considerably with irradiation temperature for ceramics such as alumina and magnesia as shown below in Fig. 6. The difference may result from the size of the collision cascade which is thought to be compact for high Z metals (Fig. 7), whereas recent computer simulations of a collision cascade in $MgAl_2O_4$ spinel show a more extended series of collisions as shown in Fig. (8).

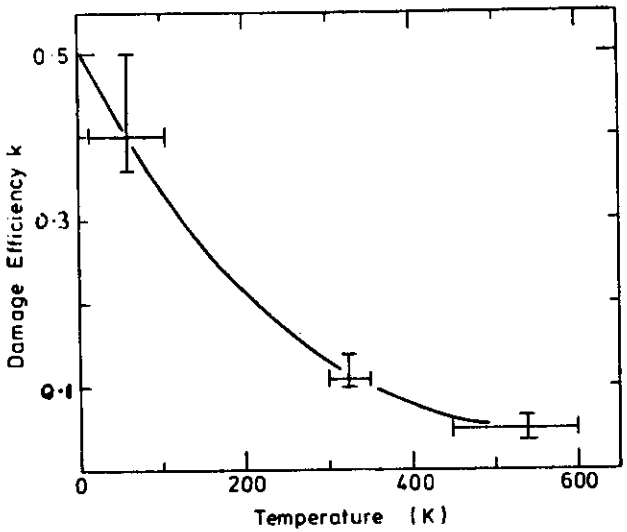

Fig. 6 Displacement damage efficiency as a function of temperature for magnesium and aluminium oxides derived from data in refs. [10–15,20,23–25].

See : G.P.Pells, J. Nucl. Mat., 155-157 (1988) 67

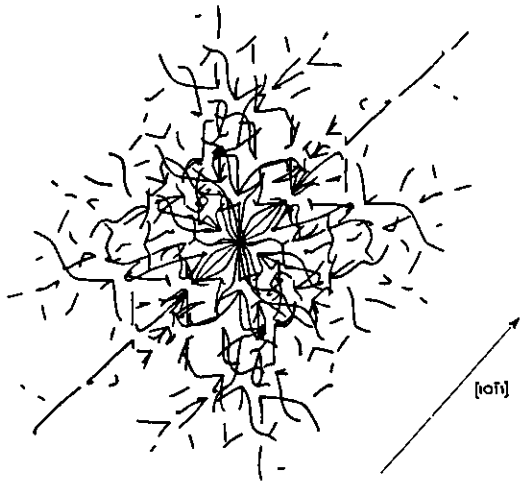

Figure 7 The 80 eV energy correlation diagram for the (1$\bar{2}$10) plane, which superimposes trajectories of the atoms in events where the primary lead atom is projected with energy 80 eV at angles varying from 0° to 360°. Strongly assisted focusing occurs in the 40° event for atoms moving in the [$\bar{1}$011] direction, but this requires projection within a small angle of this direction, otherwise defocusing takes place immediately. The relatively long range of the secondary knock-ons is a consequence of the very open lattice of lead iodide.

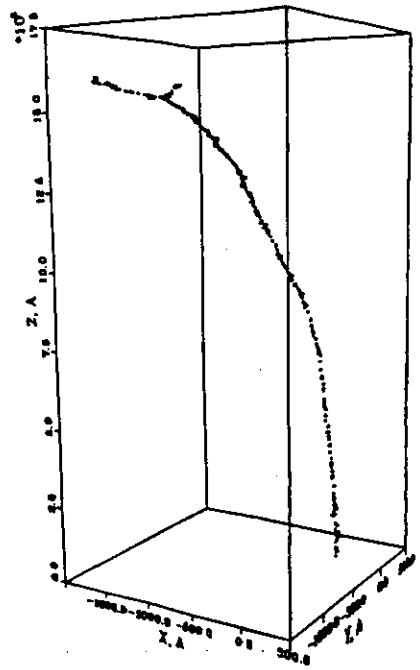

Fig. 8. Fusion neutron cascade simulation (3-D)

Defects Produced by Radiation Damage

Studies of radiation-induced defects in insulators have a considerable advantage over those in metals in that point defects, often referred to a colour centres, can be studied in some detail by optical spectroscopy and magnetic resonance techniques. In some favourable cases a combination of optical absorption and electron paramagnetic resonances measurements allow the oscillator strengths (or efficiency) for the optical transition of a particular defect to be determined and hence the concentration of centres in the irradiated solid to be easily followed. The number of possible defects types is large, therefore it is important to have a method of labelling each defect type. A self-consistent classification was devised by Sonder and Sibley. The most important points of this notation are as follows:

E. Sonder and W.A. Sibley, in 'Point defects in solids' (Eds. J.H. Crawford and L.M. Slifkin) Plenum Press 1972.

Sonder and Sibley Defect Classification

(a) The basic atomic character of the defect is represented by a letter:

F is used for negative ion (anion) vacancies
V for positive ion (cation) vacancies
I is for intersititial species

(b) The electronic character of the defect is given by a superscript charge. Thus an oxygen vacancy has an effective positive charge, since an anion has been removed from an otherwise neutral lattice, and would be designated F^{2+}. If charge neutrality was provided by the capture of two electrons in the same vacancy the defect becomes an F centre.

(c) Aggregates of point defects are written as if they were molecules; for example two neighbouring F centres is designated F_2.

(d) Impurity atoms are included as a subscript. An F centre next to an impurity atom would be called an F_A centre and a cation vacancy next to an OH^- ion and having a trapped hole in an alkaline earth oxide would be a V_{OH} centre.

Point Defects in Oxides

The nature of point defects has been extensively studied in the alkali halides over a large number of years and a modern review of the subject is given by Chadwick and Terenzi. The ideas and experimental techniques developed in the study of alkali halides was carried over to the more refractory, oxides such as alumina, magnesia and calcia. The latter have been extensively studied as model oxides and their properties are fully covered by Henderson and Wertz. Alumina, a more technologically important material which has received attention in recent years due to its potential use in nuclear fusion reactors, will be used to illustrate the variety of defects that may be produced by radiation damage.

A. V. Chadwick and M. Terenzi (Eds), Defects in Solids: Modern Techniques. Plenum Press 1986.

B. Henderson and J. E. Wertz, Defects in Alkaline Earth Oxides with Applications to Radiation Damage and Catalysis. Taylor and Francis 1977.

Radiation Damage in α-Al2O3

Unlike the alkali halides the refractory oxides do not damage by radiolysis and atoms will only be displaced by direct collision with an energetic particle. Therefore neutrons of energy >1keV or electrons of energy >200keV are required to produce displacements. The majority of defect studies have been on neutron irradiated sapphire (single crystal α-Al_2O_3) and typical optical absorption spectra are shown below before and after neutron irradiation to 10^{18} n/cm^2.

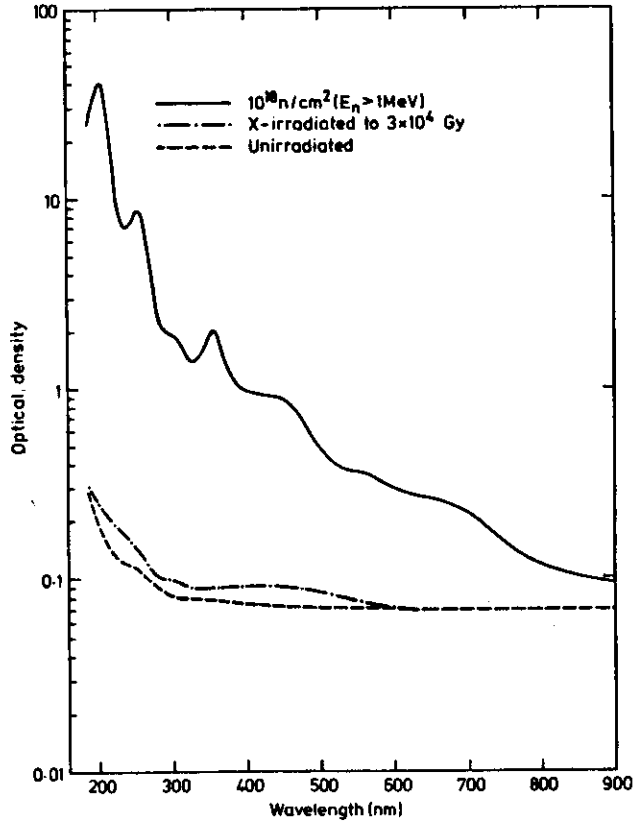

Fig. 9

The spectrum is the sum of a series of overlapping Gaussian absorption bands. The identification of the defects responsible for the observed absorption bands has been reviewed by Crawford. We will briefly follow the evolution of the optical spectrum.

Two primary defects may be observed without irradiation by varying the conditions in which the crystals are grown. An oxidising atmosphere above the melt will produce a crystal difficient in aluminium ions. As mentioned before cation vacancies maintain charge neutrality by decreasing the number of electrons on the surrounding cage of anions, in this case oxygen, to give a V centre. Clearly the neutral defect, a V^o centre, would involve the loss of 3 electrons from the six surrounding O^{2-} ions. In practise because of the balance of impurities usually present in the crystals the stable defect is a V^- centre, that is only two electrons are missing from the surrounding oxygen ions. The V centres are optically active giving a broad absorption band which peaks at 400nm.

J.H. Crawford, J. Nucl. Mat., 108-109 (1982) 644-654.

If the crystal is grown under a reducing atmosphere then it will be oxygen deficient. Again to maintain charge neutrality the oxygen vacancy will trap one or two electrons to give an F-type centre. If only one electron is trapped then the vacant lattice site is still deficient in negative charge and is therefore designated on F^+ centre. A full complement of two electrons gives the F centre with an optical absorption band peaking at 205nm.

Irradiation with low doses of neutrons will lead to discrete collision cascades producing mainly V and F-type centres. Their concentrations increase linearly with neutron dose as shown by the linear variation of optical density of the F and V absorption bands with neutron fluence, (Fig. 10).

It should be noted at this point that the area under an absorption band is directly proportional to the number of defects in the sample and may therefore be used as a measure of defect concentration N were

$$N = \frac{0.87 \times 10^{17}}{f} \cdot \frac{n}{(n^2+2)^2} \cdot \frac{(O.D.)}{d} \cdot w \qquad (19)$$

This is usually called Smakula's formula where f is the oscillator strength of the absorption band, n is the refractive index at the peak of the band of optical density (O.D.) d is the thickness of the sample and w is the band width at half-height in eV.

Neutron irradiation to higher doses will eventually lead to the point where collision cascades begin to overlap. The overlapping defect volumes increase the probability of adjacent, similar defects forming defect aggregates and also of adjacent interstitials and vacancies leading to defect recombintion. The latter clearly reduces the total number of defects in the crystal and as the irradiation proceeds the continual production of new point defects will be opposed by both defect recombination and aggregation until a state of dynamic equilibrium will be attained and the concentration of simple point defects will saturate at a fractional concentration of $\sim 10^{-3}$.

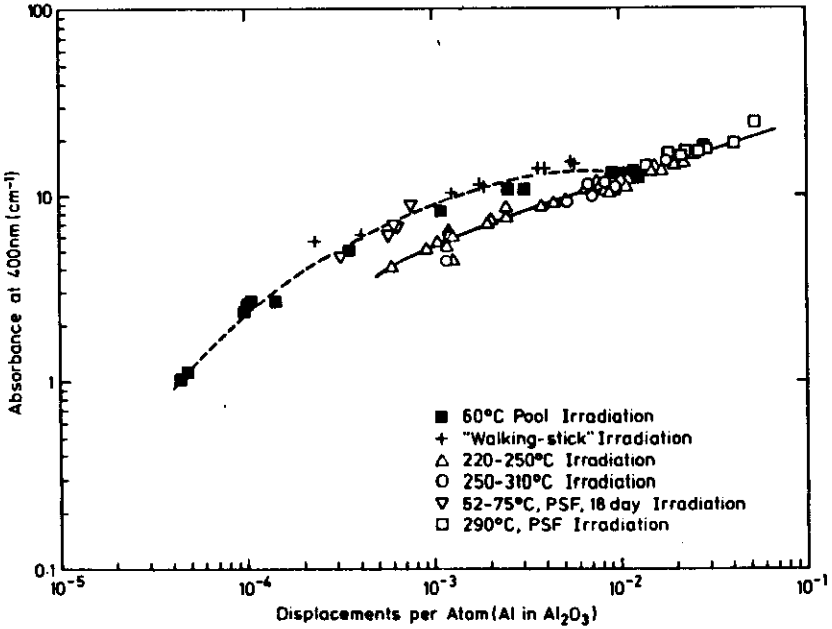

Fig. 10.

The energy levels in eV at which trapped electrons occur within the band gap of sapphire has been deduced for some simple defects as shown in Fig. 11 below.

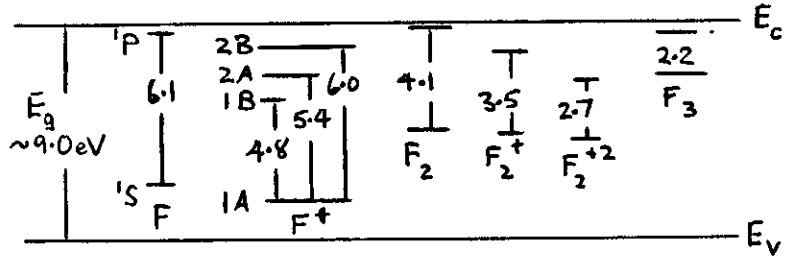

The electronic structure of the one-electron F^+ centre and the two-electron F centre are hydrogen- and helium-like (1s) and $(1s)^2$ configurations. The low symmetry of the latter splits the excited p state, which would be triply degenerate in an isotropic environment, into three states designated in order of increasing energy as 1B, 2A and 2B. Hence three transitions from the 1A ground state are expected. For electric dipole transitions only σ transitions are allowed for A-A and only π transitions for A-B thus allowing the use of polarised absorption and luminescence measurements to identify the various transitions of the F^+ centre.

Similarly the optical anisotropy of sapphire has allowed the orientation of some of the F-aggregate centres to be determined from the transition dipole moment of the defect with respect to the c-axis. A typical polarised absorption spectrum is given in Fig. 12 from which it was deduced that the 350nm absorption was an F_2 type centre with the two next nearest oxygen vacancies lying in adjacent basal planes. Similar studies have shown that the 550nm band is an F_3-type centre with the three adjacent oxygen vacancies as shown in Fig. 13.

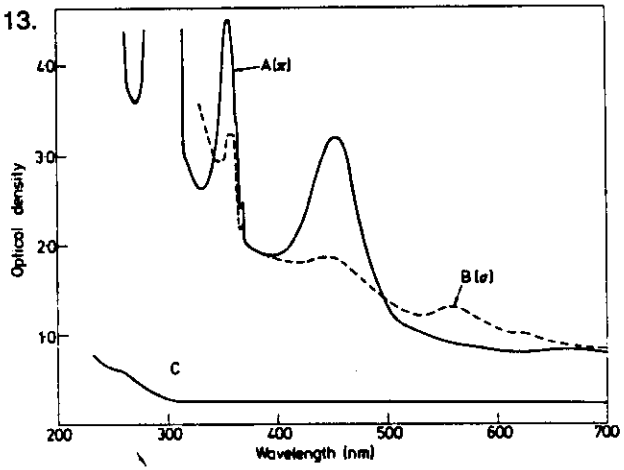

Figure12. Absorption spectra at 4 K of an α-Al_2O_3 crystal neutron-irradiated to a dose of 10^{14} neutrons cm^{-2}. The light propagates along the $[10\bar{1}0]$ axis and curves A and B refer to the same polarisations as in figure 1. Curve C is the background absorption spectrum of the crystal before irradiation.

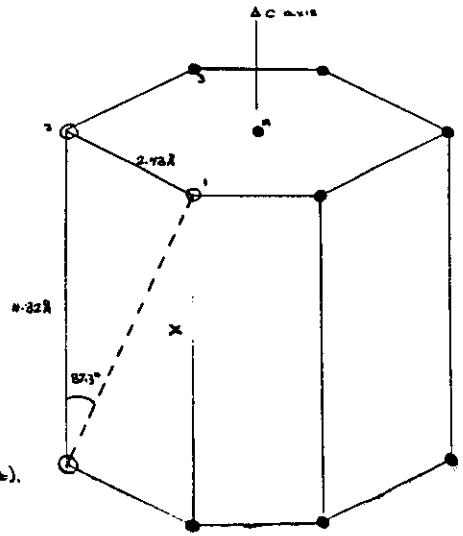

Fig 13

- oxygen ions
- oxygen vacancy
- x further possible oxygen vacancy (one level).

Interstitials

The fate of interstitials produced by radiation damage is much more difficult to determine and clues may be obtained in only a few special cases. Electron spin resonance measurements have identified Al^{2+} pairs oriented along the c-axis of sapphire and Rutherford back scattering has shown that a large fraction of displaced aluminium ion occupy the normally vacant Al lattice sites in Al_2O_3. Therefore, from these two observations it may be inferred that displaced aluminium atoms are accommodated in the normally empty Al lattice site by adjustment of the charge state of the 'intersititial' and a near neighbour. Similar adjustments of normal charge state around interstitials may have to take place in other irradiated ceramics.

Several attempts have been made to identify oxygen molecular ions in both Al_2O_3 and MgO without success which suggests that oxygen interstitials must be present as true interstitials with either no charge (the atom) or singly charged with charge adjustment on a neighbouring cation.

Defect Mobility and Aggregation

Defects become more mobile with increasing temperature either during irradiation or during post-irradiation annealing. It is generally found that interstitials move more readily than vacancies, but if the temperature is high enough vacancies also become mobile. Post-irradiation defect mobility is generally described by equations similar to those of chemical kinetics. It is assumed that a defect requires a certain energy E in order to undergo some reaction which modifies its contribution to a measured property change. The fraction of defects possessing this energy is given by a Boltzmann factor exp [-E/kT]. The annealing rate of a property P is then assumed to be described by

$$\frac{dP(t)}{dt} = -AP(t)\exp\left[-\frac{E}{kT}\right] \qquad (21)$$

where P(t) is the property change remaining after time t at temperature T in degrees Kelvin. It should be noted that the activation energy E is for defect motion and does not include a defect creation term.

Aggregation During Irradiation

As mentioned before, as radiation dose increases defects can recombine athermally within some small volume of the order of few lattice diameters. Considering the recombination volume v alone yields the approximate result for the fractional defect accumulation kinetics c,

$$c = \frac{1}{4v}\ln(4vKt) \qquad (22)$$

where K is the forward rate of defect production in dpa/s.

Purely statistical recombination within an increasing total recombination volume leads to slowly saturating kinetics (curve 1, Fig.14) significant overlap of individual recombination volumes after these kinetics; overlap can occur by statistical aggregation at low temperatures or by thermally activated defect migration. If only one defect species aggregates significantly, for example interstitials in an intermediate temperature regime, the defect accumulation kinetics alter to more quickly saturating behaviour,

$$c = \frac{1}{p}\ln(pKt) \qquad (23)$$

as shown in curve (2) of Fig14.

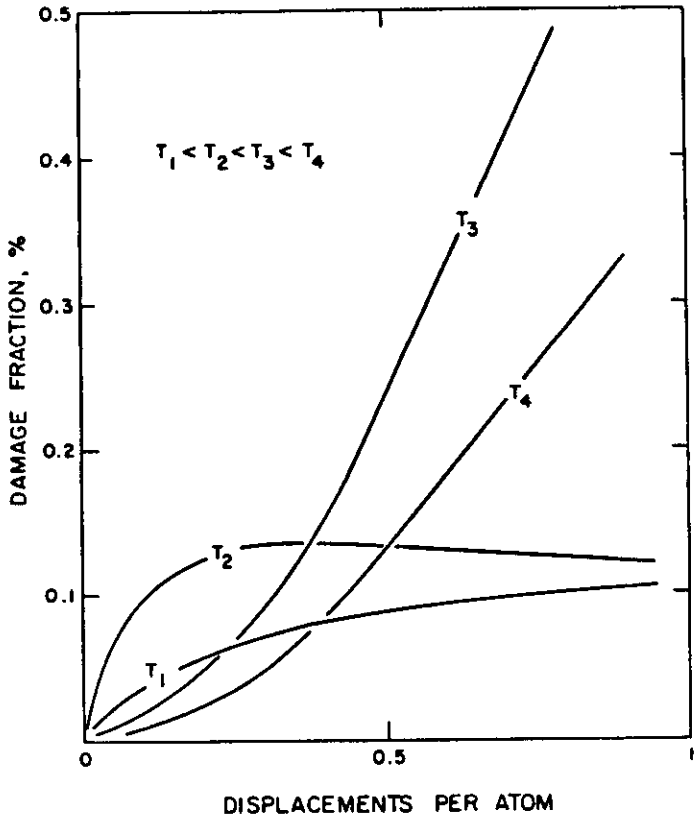

Fig. 14

Certain aggregate forms, such as dislocation loops which possess long range strain fields, generate larger athermal aggregation volumes and will also bias aggregation towards intersitital defect species. When all defects become sufficiently mobile to reach such sinks the bias effectively segregates complementary vacancy and interstitial species to respective sinks and defect content eventually accumulates linearly with dose

$$c \approx Kt \qquad (24)$$

as shown in curve (3) of Fig14 until other back reactions promote more efficient recombination.

At higher temperatures, reversible defect sinks may become unstable and defects redissolve leading to a lower accumulation rate (curve (4)) in Fig. 14). In this regime defect kinetics may be dictated by the most slowly migrating species.

Information about defect mobility derives from two sources: mass diffusivity measurements and defect aggregation kinetics. An example of defect aggregation kinetics is given in Fig. 15 where the migration of F centres in sapphire to form F_2 centres was used to determine that the activation energy for short range diffusion of oxygen vacancies in Al_2O_3 is 0.55eV.

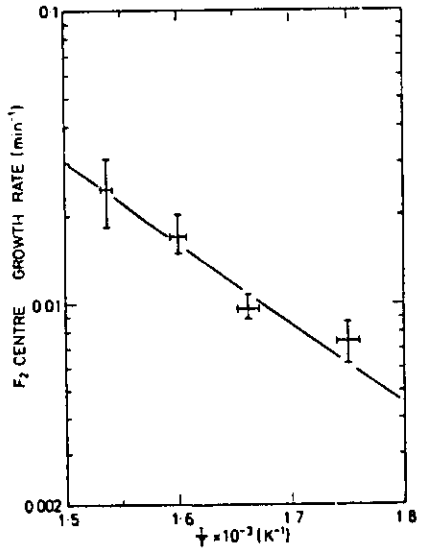

Fig 15

Planar Defect Aggregation

Radiation defects seldom exist in isolation because of their strain or Coulomb fields which drive them towards mutual aggregation or annihilation. Singificant defect motion can occur without apparent thermal activation over short distances and of course rcombination and aggregation both occur within dense displacement cascades and during cascade overlap. The aggregates formed within collision cascades and at cascade overlap are thought to form the nuclei for subsequent defect growth involving long range thermally-activated migration of point defects.

The aggregation of point defects leads to the formation of two- or three-dimensional extended defects (dislocation loops and voids). The activation energy for motion of point defects in oxides is typically 1-2eV where transport is usually ascribed to fully ionised oxygen vacancies. There is little information on the motion of interstitials.

In ceramics it is usually found that only interstitials aggregate into dislocation loops. Vacancies are occasionally observed to form voids.

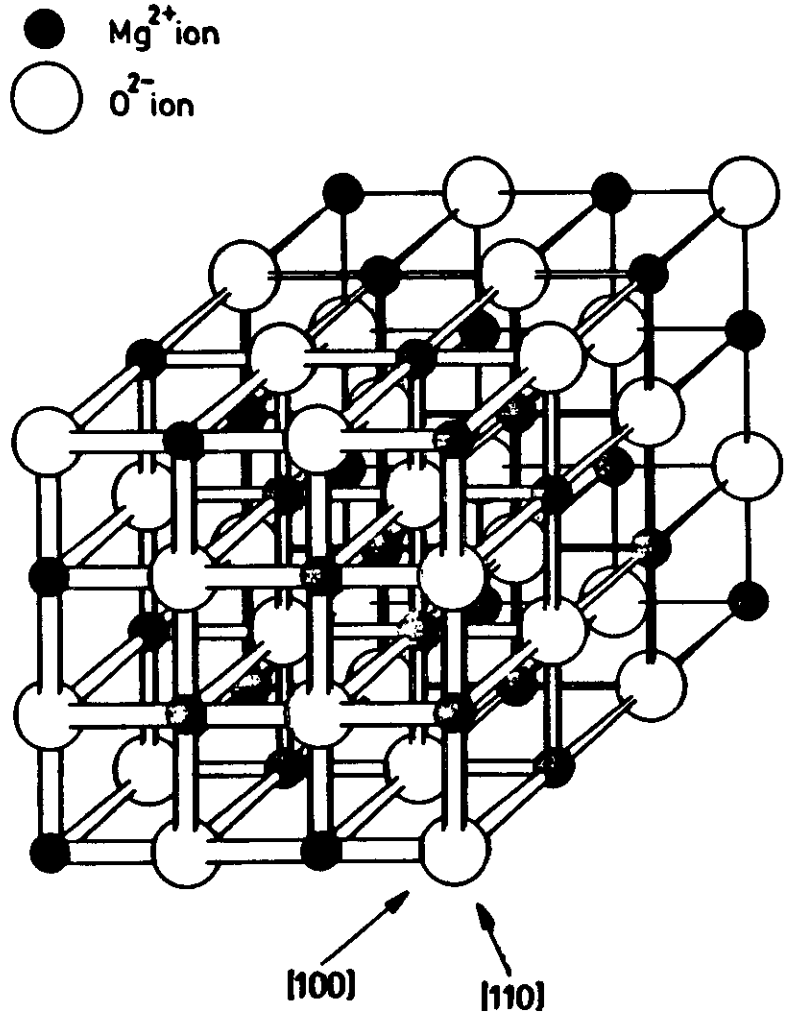

Figure 16

Dislocation loops

The nucleation of dislocation loops serves to redistribute the short-range accommodation strain of interstitials into a long-range strain field whose elastic energy per added interstitial decreases with increasing loop size. In polyatomic materials the conditions for interstitial condensation require that both stoichiometry and sublattice order must be preserved. This may be illustrated in the case of MgO which has the f.c.c. rocksalt structure which may be thought of as two interpenetrating simple cubic lattices of Mg and O (Fig. 16). Radiation leads to the formation of two-layer abab, b = <110>{110} loops, each layer of which is stoichiometric and unfaulted (Fig. 17).

Dislocation loops grow by non-conservative propagation of jogs which may be of different character at different places around the loop perimeter. The elongated loop morphology accelerates loop interaction and the formation of dislocation networks.

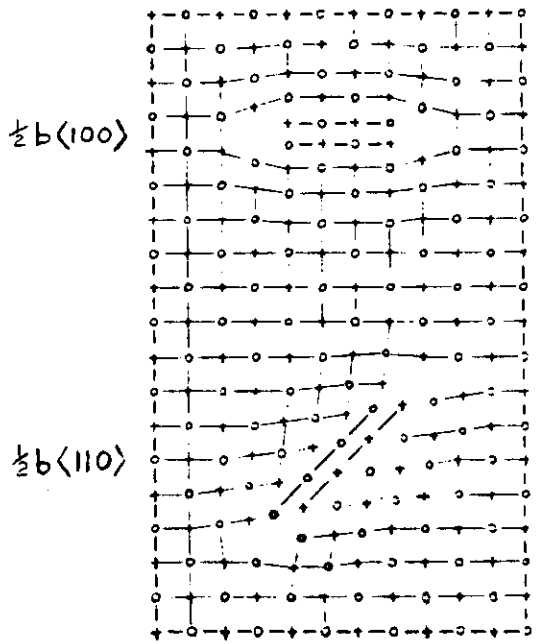

Fig. 17

In materials with less simple structures than MgO the complexity of the crystal structure may lead to the nucleation of loops which are initially faulted in order to minimise strain energy.

Irradiation of alumina leads to the formation of $\frac{1}{3}[0001]$ or $\frac{1}{3}[10\bar{1}0]$ dislocation loops on the basal {0001} and prismatic $\{10\bar{1}0\}$ planes respectively that are stoichiometric but faulted on the aluminium sublattice. It has been shown that it is not necessary for aluminium and oxygen to be displaced in stoichiometric numbers for stoichiometric loops to form as cation interstitials may precipitate between basal or $\{10\bar{1}0\}$ planes and with simultaneous diffusion of oxygen ions into the aluminium layers produce the same faulted loops. With further irradiation either loop may unfault at a critical size of ~100nm by the passage of a $\frac{1}{3}<0001>$ or $\frac{1}{3}<10\bar{1}0>$ partial shear across the loop plane. The resulting $\frac{1}{3}<10\bar{1}1>$ unfaulted lops are free to rotate and therebye become more energetically favourable sinks for further absorption of interstitials. Their further growth leads to intersection and the generation of dislocation networks after ~0.3 dpa.

Voids

Vacancy aggregation or voids form within the temperature range 0.3-0.6 T_m where T_m is the temperature of melting in degress absolute. Below 0.3 T_m vacancies are not sufficiently mobile to aggregate and above 0.6 T_m a void if it existed would become a source of thermally generated vacancies and so would shrink. There are two other necessary conditions that must be fulfilled before voids can form. The first is that an interstitial dislocation network or other interstitial sink is available to provide a biased trap for interstitials. Secondly the surplus vacancies require the presence of a gaseous impurity to help nucleate a void. Reactor irra. ation will produce helium as a transmutation product which is then available to stabilise void nuclei although there is usually sufficeint hydrogen in ceramics to serve this purpose.

Voids have been observed in MgO, α-Al_2O_3 and $MgAl_2O4$. In α-Al_2O_3 the voids tend initially align in rows along the c-axis and at high damage doses to eventually form three dimensional hexagonal arrays. Polycrystalline $MgAl_2O_4$ forms voids along grain boundaries which act as interstitial sinks but not within the grains.

Under certain irradiation conditions colloids may form such as occurs in neutron irradiated Li_2O. Electron irradiation of α-Al_2O_3 also forms colloids at high doses but in this case voids form first and subsequently trap aluminium interstitials which, due to the low displacement threshold energy of Al in Al_2O_3, are produced in greater numbers than oxygen interstitials.

Colloids are more usually formed as a result of the aggregation of anion vacancies which in a diatomic solid leaves a cationic rich volume which collapses to form a colloid. The colloids grow by trapping anion vacancies. The growth has been followed in some detail in the alkali halides because of the ease with which they may be detected by optical spectroscopy due to Miei scattering. The formation of colloids in irradiated insulators has been reviewed by Hughes.

A.E. Hughes, Rad. Effects, 74 (1983) 57-76.

Structural Effects of Radiation Damage

There have been extensive reviews of the effects of radiation on the physical and mechanical properties of ceramics as listed below. However, there are still many properties for which data is scarce and in some areas non-existent until very recently when world-wide interest in fusion power created an interest in the radiation damage behaviour of electrical insulators and lithium based ceramics for tritium breeding. So, although there is a reasonable body of information on dimensional stability there is little on the statistics of fracture.

R.S. Wilks, J. Nucl. Mat., 26 (1968) 137.

L.H. Rouner and G.R. Hopkins, Nucl. Technol., 29 (1976) 274.

F.W. Clinard Jr., J. Nucl. Mat., 85 and 86 (1979) 393.

G.P. Pells, J. Nucl. Mat., 122 and 123 (1984) 1338.

F.W. Clinard and L.W. Hobbs, in: Physics of Radiation Effects in Crystals, Eds. R.A. Johnson and A.N. Orlow (Elsevier, Amsterdam 1986) p.387.

Swelling

At low temperature many defect survive in isolated form. Lattice dilation associated with a Frenkel pair is usually positive so that their presence results in an expansion. An important exception is $MgAl_2O_4$ spinel which may compact or expand depending on the irradiating species. Growth is typically limited to a few volume percent as defect concentration reaches saturation and rates of generation and recombination become equal. Dilational swelling is often measured by X-ray diffraction methods. However, in heavily irradiated ceramics it is found experimentally that bulk and X-ray swelling may differ significantly. Thus macroscopic swelling measurements by immersion or dilatometric methods are preferred.

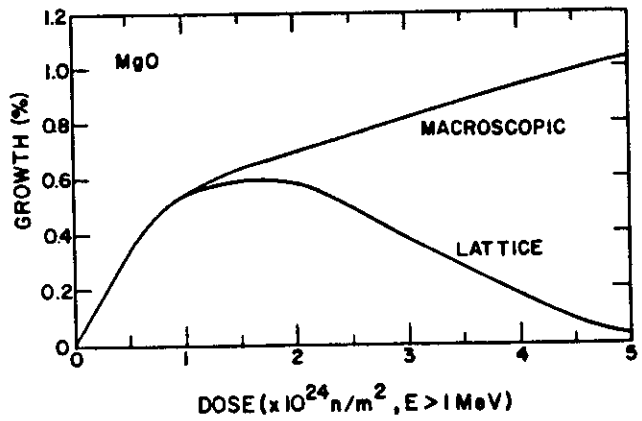

Fig. 18. Swelling growth of MgO as a function of neutron dose at 348–373 K (Hickman et al. 1966).

At intermediate temperatures, vacancies remain immobile but interstitials move to sinks or recombination sites. Under these conditions irradiated material may contain vacancies plus a dense array of interstitial dislocation loops or tangles. The dislocation loops represent the addition of new atom planes to the material leading to macroscopic swelling.

At high irradiation temperatures both interstitials and vacancies are mobile, but as dislocations attract interstitials more strongly than vacancies an excess of vacancies result. Those may aggregate to form voids.

Swelling has been studied extensively in alumina and macroscopic swelling after 20 dpa is shown in Fig.19 with the swelling peak occurring at 0.55 Tm. Fig.20 presents the macroscopic swelling produced by neutron irradiation in a variety of reactor spectra for irradiation temperatures with the range 850-1050K. It can be seen that there is an initial linear increase in swelling with damage dose due to increasing concentrations of interstitials and interstitial dislocation loops. At~3 dpa the slope changes to follow a power law in which swelling varies as damage dose to the power 0.5-0.6. Such behaviour has been ascribed by Mansur to the limiting condition in which the dislocation density was constant; recombination of vacancy and interstitial was of minor importance; voids were the dominant sink and the void surface was the rate determining feature. This is consistent with the observed dense dislocation network.

L.K. Mansur, Nucl. Technol., 40 (1978) 5.

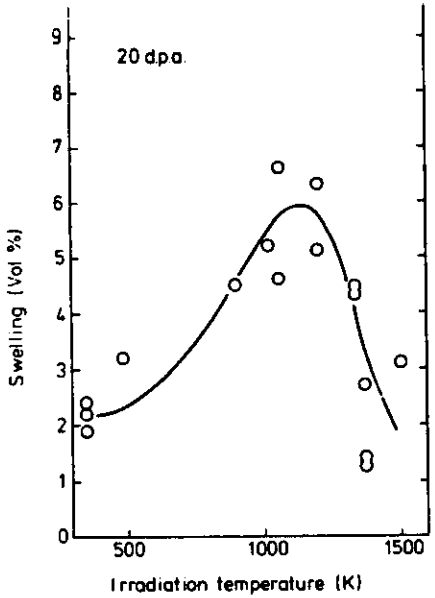

FIGURE 19
Macroscopic swelling of polycrystalline alumina as a function of temperature for a damage dose of 20 dpa taken from ref. 35

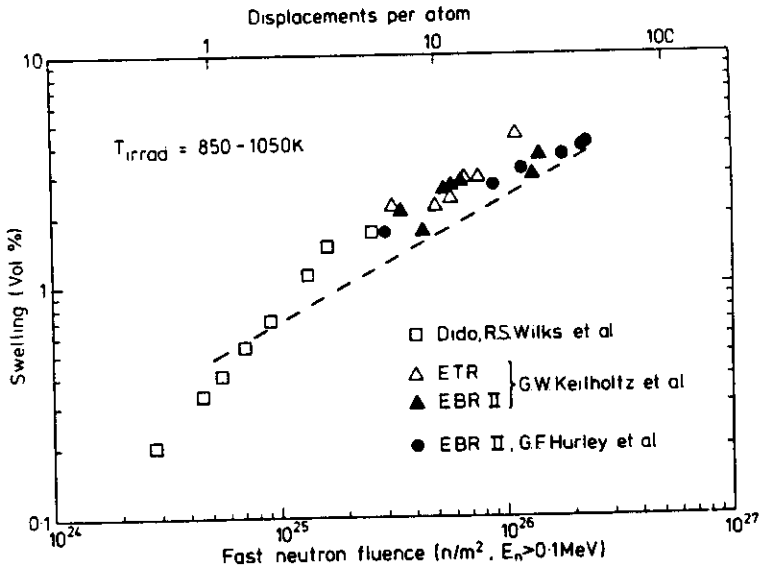

FIGURE 20
Macroscopic swelling of alumina fast neutron irradiated within the temperature range 850-1000 K as a function of neutron fluence. The dashed line is for alumina 1 MeV electron irradiated at 1070 K to equivalent dpa doses from ref. 41

Mechanical Strength

Only a limited amount of data exists on the mechanical properties of ceramics because of the high cost of reactor irradiation of large numbers of samples. In general it is found that Young's modulus decreases by 5% after 1 dpa.

Catastrophic weaking can result from anisotropic swelling leading to grain boundary cracking as demonstrated by the modulus of rupture of neutron irradiation BeO shown below. However, the modulus of rupture and elastic modulus of cubic β-SiC were not significantly changed by very high neutron doses of 1.2×10^{26} n/m^2 at temperatures of 1000 C and below. The bend strengths of the more complex reaction-bonded silicon carbide show reductions with increasing neutron dose as do polycrystalline alumina samples. These materials also show significant reductions in the Weibull modulus.

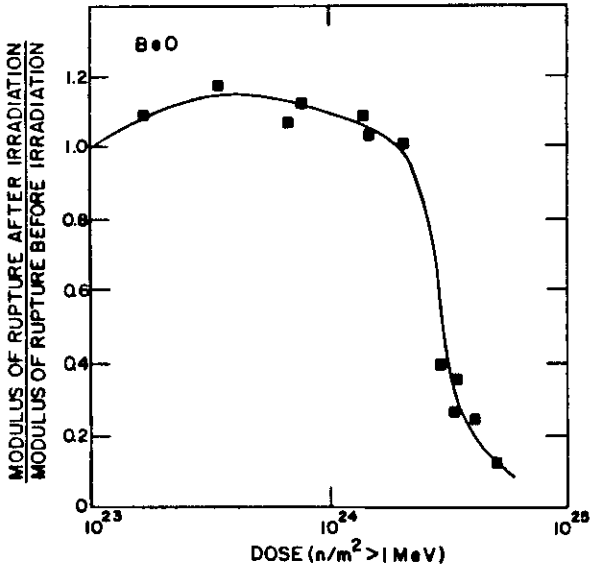

Fig. 21 Variation of modulus of rupture of BeO with neutron dose at 348–373 K.

Thermal Conductivity

In dielectric solids heat is conducted by vibrational waves (phonons) which are scattered by interacting with other phonons and with various structural defects, including those induced by radiation. The low-frequency component of the phonon spectrum is relatively sensitive to the presence of large, widely spaced defects such as grain boundaries, fault ed dislocation loops and voids. The high frequency component is most sensitive to the presence of point defects. In the limit, generalised disorder can red uce the thermal conductivity to that ofthe glassy state where the phonon mean free path is of the order of the interatomic spacing. In the more refractory oxides, neutron irradiation is found to reduce the thermal conductivity to a value no less than the lowest found as a function of temperature.

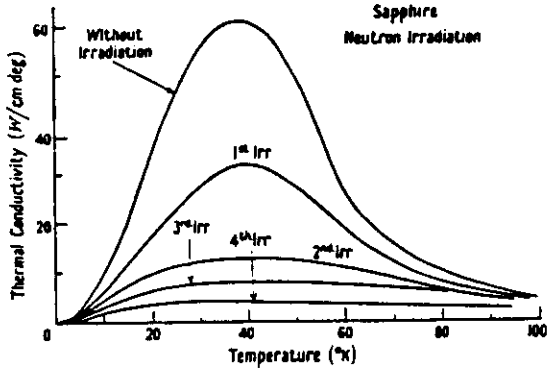

Figure 22 The thermal conductivity of synthetic sapphire before and after neutron irradiation.

Electrical Conductivity

The immediate effect of ionising radiation on an insulator is the production of electron-hole pairs by exciting electrons from the valence band, across the band gap, into the conduction band. Free holes and free electrons are thus generated at identical rates proportional to the dose rate of ionising radiation. Both electrons and holes thermalise and begin to diffuse. If an electron thermalises sufficiently close to its parent ion such that the coulomb energy is greater than thermal energies then the electron may be recaptured before contributing to conduction processes. This is referred to as geminate reecombination and occurs on a timescale of $<10^{-11}$ s. Electrons and hole that escape geminate recombination drift under an applied electric field thereby contributing to the conductivity until recombination takes place. The carrier pairs, while they are free, contribute to the conductivity by an amount

$$\Delta\sigma = e_o\left(n\mu_n + p\mu_p\right) \qquad (25)$$

where n and p are the electron and hole densities, μ_n and μ_p are their respective mobilities. In a pure insulator the 'intrinsic' mobility of an electron or hole would be dominated by electron-phonon interactions, but in real materials immobilisation of the carriers occurs by recombination at defect sites or escape to a free surface such as an electrode with recombination being the dominant effect. For simplicity it may be assumed that the electron mobility is very much greater than the hole mobility. The excited electron density during irradiation will be

$$n = K_D R \lambda_t \,/\, \nu_n \qquad (26)$$

where K_D is the number of free electrons per unit dose, R is the dose rate, λ_t is the mean free path before trapping and ν_n is the thermal velocity. Combining equation (2) and (3) gives:

$$\Delta\sigma = e_o K_D R \left(\mu_n \lambda_t \,/\, \nu_n\right) \qquad (27)$$

An approximate value for the radiation-induced conductivity (RIC) of alumina in a fusion environment may be calculated from equation (4) using the experimental values obtained by Hughes of 75 eV/electron-hole pair, an electron mobility μ_n of 3 cm^2/Vs and the relationship $\nu_u = (2kT/m^*)$. Then for an ionising dose rate of 5000 Gy/s the induced conductivity would be $\sim 1\times10^{-6}$ $\Omega^{-1}m^{-1}$ at room temperature. However, the electron mean free path before scattering and recombination will depend upon the details of the crystal structure, type of defect, composition and the interaction of the various traps and recombination centres and it is frequently found that RIC is best described by a power law with the total conductivity being given by equation $\sigma = KR^d + \sigma_o$. This relationship was first put forward by Fowler on the basis of both electron trap theory and experimental work on polymer insulators which showed that the dose rate exponent could vary between 0.5-1.0. At about the same time Rose described the recombination process in insulators and semiconductors which would lead to similar non-linear behaviour including a two-stage recombination model that could lead to supralinearity. In a later publication Rose discussed the concepts of photoconductivity in some detail.

The recombination of electron and hole via defect states in the band gap may be illustrated by consideration of the situation shown in Figure 23 in which ionisation has led to a population of thermalised electrons at the bottom of the conduction band and holes at the top of the valence band. There are states A near the conduction band such that electrons falling into these states are rapidly re-excited thermally into the conduction band. These states are in thermal equilibrium with the electrons in the conduction band and are called shallow trapping states. Electrons falling into deeper lying states B will not be thermally re-excited for a long time and before thermal re-excitation takes place, such an electron is more likely to capture a free hole. These deeper lying states will be called ground states. There are also shallow trapping states A' for holes thermally excited from the valence band. The ground states are mainly those discrete states that lie between the two steady state Fermi levels defined by the free-electron concentration and the free hole concentration created during irradiation. As the

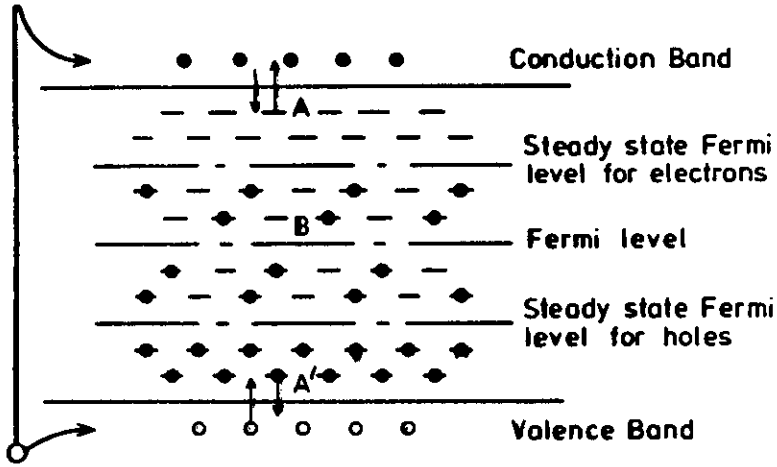

Fig. 23.

excitation is increased and free carriers increase, the two steady state Fermi levels move apart towards their respective band edges. Conversely, if the excitation is suddenly removed the free carrier densities decay in time towards zero.

A simple linear response is obtained with a set of discrete states lying near the Fermi level. These below the Fermi level are essentially filled with electrons and those above are essentially empty. Under ionisation conditions electrons excited to the conduction band must return to the valence band via the impurity ground states at the same rate as holes return to the conduction band in order to maintain electrical charge balance. Fractional powers between 0.5 to 1.0 can be accounted for by a model which assumes a quasi-continuum of discrete states. As excitation is increased the steady state Fermi levels draw apart and include a larger number of ground states. The larger number of ground states shorten the lifetime of the free carriers and thereby lead to fractional powers of conductivity as a function of dose rate.

Rose proposed a model for $d > 1$ involving electron hole recombination centres in which the hole centre has an extended range of electron states within the band gap. Hole trapping at this centre releases electrons to the electron trap thereby sharply reducing the ability of the electron trap to capture electrons from the conduction band. Therefore the lifetime of electrons in the condution band is extended. As the dose rate is increased the Fermi levels in the hole trap move apart and so increasingly transfer electrons to the other trap leading to a supralinear conductivity-dose rate relationship.

A. Rose, "Concepts in Photoconductivity and Allied Problems" in Interscience Tracts on Physics and Astronomy No. 19 (1963).

A.C. Propagation at High Frequencies

When a ceramic is employed as a dielectric window or a capacitive insulator it can be shown that the power loss from an ac wave appearing as heat within the material is given by

$$P = \omega \epsilon_0 \epsilon' \tan\delta E^2 \quad W/m^2 \qquad (27)$$

where ω is the frequency of the alternating electric field E, ϵ' and ϵ_0 are the permittivity of the material and free space, respectively. The dielectric loss, $\tan\delta = \epsilon''/\epsilon'$, is the modulus of the ratio of the real and imaginary parts of the relative permittivity. There are three major polarisation mechanisms in solids. The electron cloud surrounding the nucleus of an atom will oscillate in an ac field causing the centre of charge to behave like an oscillating dipole and because of the low inertia of the electrons can operate at all frequencies up to the visible part of the electromagnetic spectrum. At infrared and microwave frequencies molecular mechanisms become operative when the centres of positive and negative charge between two different atoms do not coincide thus creating a dipole which, under the influence of an electric field, will oscillate giving rise to a polarisation mechanism. There will also be many defects which can trap charge. The accumulation of charge at a point within a solid will cause an image charge of opposite sign to be induced on an electrode thereby creating a dipole.

There has been few experimental results and even less theoretical consideration on the effects of radiation on dielectric loss mechanisms although Pells and Hill [70] have pointed out that radiation-induced dc conductivity will make a contribution to ac loss which will be inversely proportional to frequency. It should also be pointed out that the industrial manufacture of low loss ceramics ($\tan\delta < 10^{-4}$) is difficult and still remains more of an art than a science. Therefore it must be expected that, of the many types of defect that are produced by radiation damage, some will have a dipolar nature leading to a dielectric loss. Displacement damage will produce vacancies and interstitials at concentrations which saturate at ~1000 appm. The location and charge state of the interstitials are unknown but they may occupy such positions as to produce interfacial or molecular dipoles. Transmutation products may also contribute to an increase in loss, particularly the highly mobile species hydrogen and carbon.

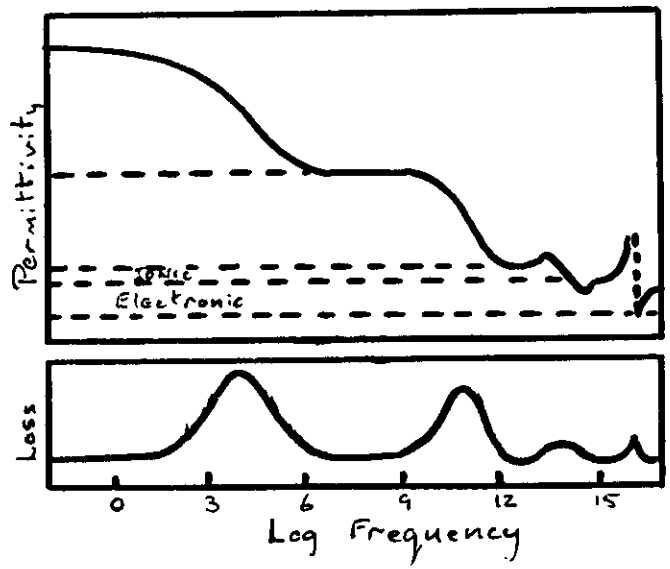

Fig. 24

Applications

As may be expected the principal application of radiation and ceramics is within the nuclear power industry.

Nuclear Fission

If one considers the dominant reactor type in use throughout the world - the pressurised water reactor - then the use of ceramics is quite minor as their operating temperature is only 290 C. There may be a few mineral insulated control cables. Reactors operating at higher temperatures such as the Advanced Gas-cooled Reactors in the U.K. and the various fast breeder reactors have to use ceramic fuel, in most cases UO_2 or $(U, Pu)O_2$. The higher operating temperature of the AGR (600 C) also requires that alumina spacers are inserted at each end of the fuel rod to stop chemical reactions between the fuel rod and the stainless steel fuel can. The reactor control rods are also ceramics such as Eu_2O_3 or Gd_2O_3 which have high neutron capture cross-sections. Several experimental high temperature gas-cooled reactors have been built to work at 1000 C with hot zones constructed largely of ceramics. In this case the fuel is UC spheres encapsulated in SiC.

The fission of ^{235}U yields three neutrons of average energy 2MeV and two fission products of ~100MeV. The neutrons have mean free paths of ~1cm and so have little impact on the fuel but the high energy fission fragments have a range of only a few tens of micrometers and so deposit all of their energy within the fuel creating intense displacement damage. Gas generated during fissioning (He, Xe, Kr, I) are mostly insoluble and precipitate both intra- and intergranularly as gas bubbles. Such bubbles attract vacancies to relieve the surrounding stress fields, so that gas-filled voids are made up primarily of vacancies. Bubbles often migrate up a thermal gradient towards the centre of the fuel rod. Solid transmutation products may also migrate along thermal gradients and precipitate out as separate compounds.

Nuclear Fusion

The vertical cross-section of most tokamak reactor designs shows a series of concentric layers broached by a number of radial apertures. Each layer maycontain ceramic material to a greater or less extent depending upon the detailed operating conditions of the particular design. The most severe conditions naturally occur at the innermost layer facing the plasma where a neutron wall loading of 1 MW/m^2 gives a total neutron flux of $3.6x10^{18}$ $n/m^2/s$. There will also be other radiation impinging on the first wall such as X-rays and fast particles. Therefore, as radiated heat loss from the plasma due to impurities varies as Z^{3-7} (for $Z>6$) it is generally proposed that a metal first wall will have to be protected by a refractory, low Z material.

Fixed and moveable limiters which project into the plasma may have to withstand heat loads of over 10 MW/m^2, and therfore highly refractory materials of good thermal conductivity will be required. If additional heating by neutral beam injection is used then first wall armour plates may be required to give protection from neutral beam 'shine-through'. Both limiters and wall armour will need to be of low Z materials in order to minimise the effects of plasma contamination. Also within the region of the first wall there may be diagnostic windows and large antennae for ion-cyclotron resonance heating exposed to the same neutron and thermal fluxes.

Moving away from the plasma the next layer in the tokamak structure is the blanket with a total neutron flux at the centre of 10^{18} $n/m^2/s$ (referred to a front wall neutron loading of 1 MW/m^2). The function of the blanket is to extract energy from the fast neutrons produced by the fusion reaction and to provide the reaction space for tritium breeding using lithium ceramic breeders. Other ceramic materials such as graphite and silicon carbide may find application as structural members in the blanket not only for their high temperature properties but as neutron reflectors which, beign low Z materials, have the additional advantage of producing

low levels of long-lived, radioactive transmutation products. Other ceramic applications may be found in the blanket layer such as dielectric windows for r.f. heating systems and ceramic insulation for poorly shielded divertor coils.

If the blanket operates at high temperature then it may be found necessary to provide a thermal insulation layer to reduce heat transfer between the blanket and the shield. This would also be a convenient distance from the plasma, with the neutron flux down to ~$2x10^{17}$ $n/m^2/s$ and moderate temperatures, to introduce the electrically insulating torus break, as proper coupling of magnetic fields to the plasma require that the electrical continuity of a metallic torus be interrupted by a high resistance torus breaker.

The shield is the outermost layer and provides neutron and gamma-ray attenuation, where the neutron flux is reduced from 10^{17} to ~10^{15} $n/m^2/s$ by neutron absorbers such as $^{10}B_4C$.

Finally, there are the ceramic components associated with the radial penetrations of the torus structure. These are mainly concerned with plasma heating. In hybrid and electron cyclotron resonance heating systems the power is delivered along r.f. waveguides from an r.f. generator probably located outside the reactor building. r.f. windows will be required in the waveguides for several reasons. The need for high power transmission may dictate that the transmission ducts be filled with a dielectric gas such as SF_6, in which case an r.f. window is required at the reactor end. A second window placed in the blanket region may also be required to minimise the tritium inventory and in some designs an aid to smooth power transmission. The ceramic windows in the blanket region would operate at the blanket temperature and neutron flux. The electrical insulators of the ion source for neutral beam injectors would also be outside the reactor and heavily water cooled, but neutron streaming down the neutral beam line would give fluxes at the ion source of ~$2x10^{14}$ $n/m^2/s$ and an ionising flux of ~10 Gy/s.

Nuclear Waste

Reprocessing of nuclear fuel to recover fissionable materials generates a waste which must be incorporated into a solid form known to be stable over geologic times of perhaps 10^5 years. A major source of waste instability is self-irradiation damage which may lead to swelling and microcracking, the reduction of thermal conductivity and alterations to the microstructure. This may increase storage temperatures and thermal stress and to an increase in area exposed leachants. The source of self-irradiation in nuclear waste is radioative decay. Most displacements result from alpha-decay of actinide isotopes producing 5MeV alpha-particles and ~100keV in the recoil nucleus.

A number of solids have been proposed as carriers for active waste including glass and crystalline ceramics. The ceramic waste-forms go under the generall name of SYNROC which is a mixture of phases including zirconolite, perovskitie and Ba-hollandite. The zirconolite, $CaZrTi_2O_7$, and perovskite, $CaTiO_3$, serve as the principal hosts for actinides, while hollandite, $BaAl_2Ti_6O_{16}$, accommodate caesium. Radiation damage from self-irradiation, neutrons and other particles show that zirconolite becomes amorphous after ~1 dpa. Differential swelling is the major problem on SYNROC which leads to grain boundary cracking and enhanced leach rates. The most desirable form of waste storage medium would be a single phase cubic material and spinel has been proposed.